

Influence of intraocular scattered light on lightness-scaling experiments

W. Alan Stiehl, John J. McCann, and Robert L. Savoy*

Vision Research Laboratory, Polaroid Corporation, Cambridge, Massachusetts 02139

Received April 1, 1983

Following Munsell's bisection procedure [J. Opt. Soc. Am. 23, 394 (1933)], we established a nine-step gray scale in which each step is an equal increment in lightness. We calculated retinal illuminances after intraocular scatter by using the point-spread function of Vos *et al.* [Vision Res. 16, 215–219 (1976)]. After this correction for intraocular scatter, we find a logarithmic relationship between retinal illuminance and achromatic lightness scales that are determined by the bisection method. Additional bisection experiments with a series of different backgrounds corroborate this result. We find that lightness depends linearly on the logarithm of scatter-corrected retinal illuminance, with different slopes for backgrounds of different lightness. This study also highlights the importance of using scatter-corrected illuminance in any quantitative model of lightness.

INTRODUCTION

Numerous experiments have studied the relationship between luminance and sensation. This paper is concerned with the set of sensations that vary from white through gray to black. These sensations, called achromatic lightnesses or gray scales, have been studied by Munsell *et al.*,¹ Ladd and Pinney,² Glasser *et al.*,³ Stevens and Stevens,⁴ Jameson *et al.*,⁵ and Semmelroth.⁶ In these studies *lightnesses*, the sensations generated by the visual system, are compared with relative *luminances*, measures of the amount of light coming from objects to the eye. We make luminance measurements of different areas by placing a telephotometer at the eyepoint of the observer. We define such measurements as luminance at the eyepoint. A more-relevant physical quantity for models of the psychophysics of human vision is the amount of light arriving at the retina. By accounting for the physical effects of the scattering of light passing through the ocular media, we have calculated the relative stimulus at the retina. For the sake of comparison, we calculate the convolution of the luminance at the eyepoint with a selected point-spread function (PSF) from Vos *et al.*⁷ to determine the effects of intraocular scatter. We define the result of this calculation as retinal luminance.

The experiments and calculations in this paper examine the influence of intraocular scatter on lightness scales.

METHOD

Derivation of Lightness Scale

Figure 1 is a diagram of a transparent target that we call a standard lightness display. We use this display in lightness-matching experiments. A similar target and its use have been described by McCann *et al.*⁸ Our standard lightness display was obtained by using a bisection procedure similar to Munsell's procedure. Observers selected equal lightness steps by choosing from a series of neutral filters of various densities on a light box with a luminance of 3426 cd m^{-2} . First they chose a filter that appeared midway in sensation

between white and black (assigned lightnesses of 9.0 and 1.0, respectively) and labeled this middle gray area with a lightness value of 5.0. Then the observers bisected the sensations of white (9.0) and middle gray (5.0); this lightness was labeled 7.0. Then they bisected the sensations of 5.0 and 1.0 to get 3.0, 9.0 and 7.0 to get 8.0, etc. The averages of the energies chosen by several observers determined the optical densities of the seven areas with integral values of lightness in the standard lightness display. The luminances of the remaining shaded areas in Fig. 1 were interpolated along a smooth curve used to fit the nine integral values. The standard lightness display was constructed with these extra steps to facilitate the observer's judgment in lightness-matching experiments.

The luminances of the areas in Fig. 1 that are labeled 2.0–9.0 are plotted as filled circles in Fig. 2 (the opaque area, labeled 1.0, cannot be represented on this logarithmic scale). These areas are equally spaced in lightness. The values of luminance are normalized to the luminance of the white area (lightness of 9.0). The solid curve is a power law with an exponent of $1/3$ and conforms to published lightness scales.^{2,3} The luminance data conform to this power law.

Our goal was to determine the extent to which the functional form of the curve relating luminance and lightness is altered by considering the effects on luminance of intraocular scatter. We convolved the entire two-dimensional spatial distribution of luminance from the 30-by-25-deg target with the PSF of the eye to determine the pattern of illuminance at the retina.

Scatter Calculation

We used the PSF summarized by Vos *et al.* The PSF is the foveal image of a point source; this image is degraded because of optical aberrations⁹ and intraocular light scattering. Bartley¹⁰ indicates a pupil size of 2.1 mm for a luminance of 3426 cd m^{-2} , and we selected the PSF for the 2.0-mm pupil for these calculations.

The convolution is performed with an angular resolution of $1'$, the separation of retinal receptors in the fovea. There are 2,700,000 points at $1'$ separation in a 30-by-25-deg field,

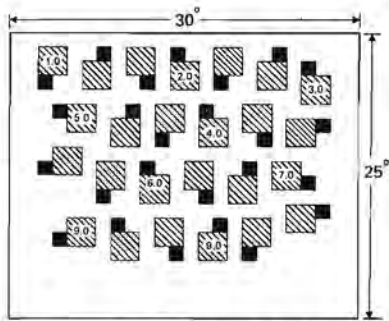


Fig. 1. Diagram of standard lightness display. The change in lightness from any one area (shaded in this diagram) to the next is constant. The sequence of areas extends along the serpentine path from black (lightness value, 1.0) to white (lightness value, 9.0); the areas with integral values of lightness are labeled. The actual labels on the display are adjacent to the areas. The 25 squares are 2.5 deg on a side in a uniform white field that subtends 30 deg by 25 deg. A small black square (1.25 deg on a side) is adjacent to each of the 25 large squares. The luminances of the 9.0 area and the background are 3426 cd m^{-2} ; the area labeled 1.0 and all the black squares are opaque. The transparency consists of a set of black papers and neutral filters of selected densities sandwiched between two glass plates.

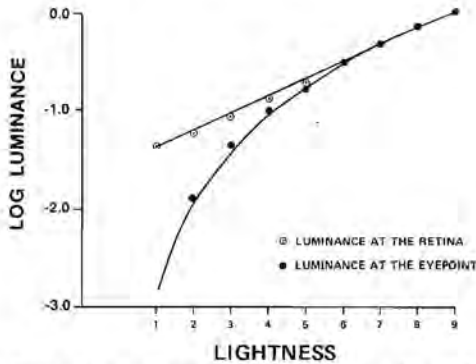


Fig. 2. Graph of relative luminances of areas selected for equally spaced increments in lightness. The filled circles are the measured luminances of the areas labeled in Fig. 1, which are equally spaced in lightness. The zero luminance of the opaque area (lightness value, 1.0) cannot be shown on this logarithmic scale. The lower solid curve is a power function with an exponent of $1/3$; the luminance data conform to this curve. The open circles are the nine calculated values of scatter-corrected luminance. Since they fall on the straight line, lightness is proportional to the logarithm of scatter-corrected luminance. Consequently, lightness is simply a linear function of the logarithm of scatter-corrected luminance as well as a power function of luminance of the target.

and the calculation of the amounts of scattered energy from so many points onto any single receptor requires about 34.5 min on our PDP 11/60. The calculation of scatter-corrected luminance at all points at full resolution would require about 177 years. We used a significant economy in calculation with no loss of accuracy for our purposes: Beyond about $10'$ from the peak, the magnitude of the scatter function begins to diminish sufficiently gradually that sampling the scatter function and the target at $1'$ intervals is not necessary. We can therefore reduce the number of samples needed for the calculation of scattered energy at a point from 2,700,000 to as few as 1304, thus eliminating over 99.95% of the execution time. Also, we do not need to determine the scatter-corrected values of luminance at all points in the retinal image, but at only a few selected ones, thereby further reducing the total execution time.

The convolution is performed in the spatial domain rather than in the Fourier-transform, spatial-frequency domain. The combination of the large display size and the high angular resolution needed to sample the inherently narrow PSF accurately makes the Fourier-transform technique unwieldy. Because we are interested in calculating the scatter at only a few points, the spatial convolution is more efficient.

We divide the source into four regions that are resolved into square areas of different sizes, with high angular resolution near the center of calculation and much coarser resolution away from it. This manner of sampling the scatter function is valid because the sizes of the different areas at each stage of resolution are chosen to be sufficiently small that the scatter function is nearly flat over each area and can be sampled accurately by the value at the center of each area.¹¹

Figure 3 depicts the different resolution sizes that are utilized to calculate the scatter-corrected luminance at an arbitrary point A on the retina. The upper diagram shows 471 square areas, each $75'$ on a side. We exclude the $225'$ region about A because the scatter function must be sampled more finely over this region. The program samples the luminances

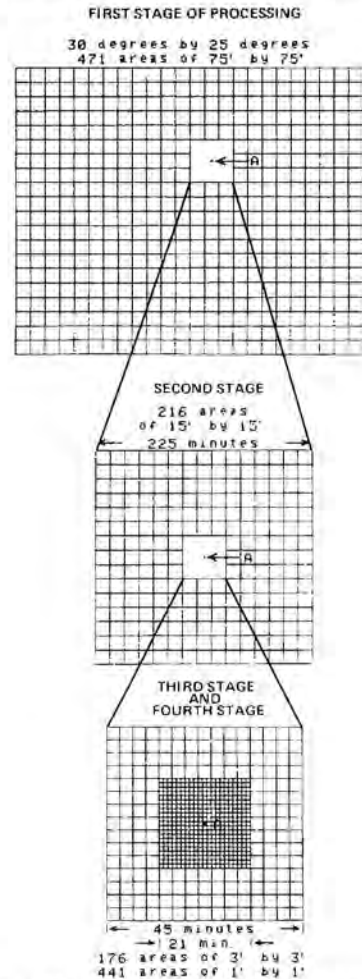


Fig. 3. Diagram of the four stages of resolution of the source for the calculation of scatter-corrected luminance. We calculate the total luminance scattered into the $1'$ square area (A) in four stages. In the first stage we calculate the scatter from distant parts of the image with a relatively coarse angular resolution. In each successive stage we calculate the scatter from areas closer to A with successively finer resolution. This technique reduces the time of calculation drastically without significant loss of accuracy.

at the centers of the 471 areas and computes the amounts of energy scattered from each of these areas to A.

In the second stage of processing, we subdivide this 225' region into 225 square areas, each 15' on a side. We exclude the central 45' region about A from this stage and compute the energy scattered onto A from each of the remaining 216 areas. In the third stage, we further subdivide the 45' region into 225 square areas, each 3' on a side. We exclude a 21' region about A and compute the energy scattered onto A from the remaining 176 3' areas. In the fourth and final stage of processing, we resolve the remaining 21' region into 441 areas, each 1' on a side, and compute the energy scattered from this final region in the same manner.

Results of Scatter Calculations

Figure 4 shows the luminance profiles, before and after scatter, along a diagonal through the middle of the black area with a lightness of 1.0 on our standard lightness display. The curves are normalized to the peak luminance of the target. The contrast between this area and its background is the greatest of the entire display, and, consequently, the effect of intraocular scatter is greatest in this area. The sharp edges in the source (the dashed lines in Fig. 4) are replaced by steep gradients, and thus there is no single value of luminance to be ascribed to this entire area of lightness 1.0. Our subsequent conclusions are the same whether we choose the value at the center of this area or use an averaging method. We used the average of the luminances at the four points on the two principal diagonals midway between the center and the four corners.

The average was calculated in this manner for each of the nine areas in the field that are labeled in Fig. 1, and these scatter-corrected luminances are plotted as open circles in Fig. 2. The effect of scatter on these nine areas is to increase the luminance in the areas of low lightness, with proportionally less increase for areas of lightness approaching that of the background. The curve plotted through these data corrected for intraocular scatter has a different functional form: a straight line when the logarithm of scatter-corrected luminance is plotted against lightness. Consequently, whereas lightness is a power function of target luminance, lightness is also a logarithmic function of scatter-corrected luminance.

FURTHER EXPERIMENTS

Procedure

We performed additional experiments to test whether the result that lightness is a linear function of the logarithm of scatter-corrected luminance can be extended to other experimental displays. We created four new targets that were designed to measure the effects of differing backgrounds on bisection lightness scales; the backgrounds were chosen to provide differing distributions of scattered light within the eye. The four targets, A, B, C, and D, are shown diagrammatically at the bottom of Fig. 5. Target A, with a uniform bright background, was chosen because the background provides large amounts of scattered light to the areas along the central horizontal axis. The background in target D is dark with a remote, thin, high-luminance perimeter; the background in D provides far less scattered light than does that in A. Targets B and C were designed to study the effects of in-

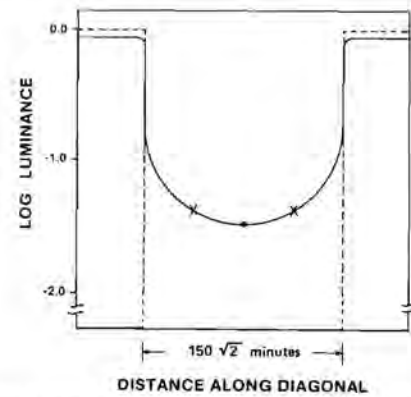


Fig. 4. Luminance profile after scatter calculation along diagonal through the opaque area in the standard lightness display with a lightness of 1.0. The dashed lines indicate the left and right boundaries of this area. The scatter-corrected luminance of this area is represented by the average of the luminances at the two points marked X and two corresponding points along the opposite diagonal. These points are midway between the center of the area (filled circle) and the four corners.

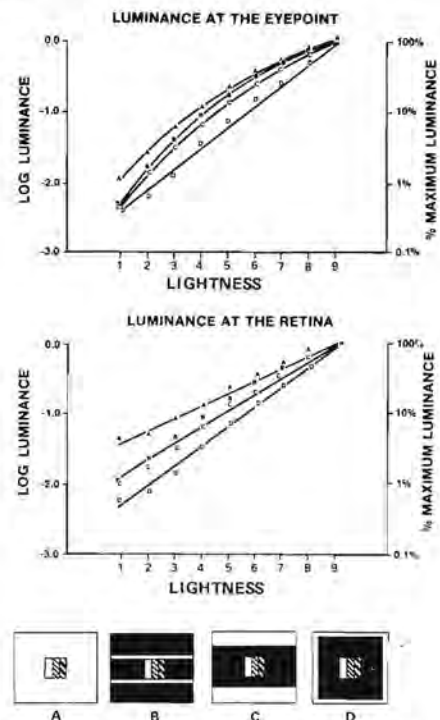


Fig. 5. Lightness scales from bisection experiments with computer-controlled video display. The four targets, A, B, C, and D, are shown diagrammatically at the bottom. The upper graph of relative luminance shows the average values of the logarithm of luminance chosen by the observers. The lower graph shows the scatter-corrected luminances. The graph shows that, for all four backgrounds, the equally spaced lightness scale is the consequence of equally spaced increments in the logarithm of scatter-corrected luminance. The slope of this linear relationship depends on the background.

intermediate amounts of scatter. In B there are thin high-luminance strips, 0.63 deg wide, adjacent to the test areas, and in C the width of the strips was increased to 2.5 deg and they were offset above and below the test areas by 1.88 deg. Both targets were designed so that the same amount of light scatters from the surround into the central test area.

Observers performed the bisection experiments on these four targets in a procedure similar to that described previ-

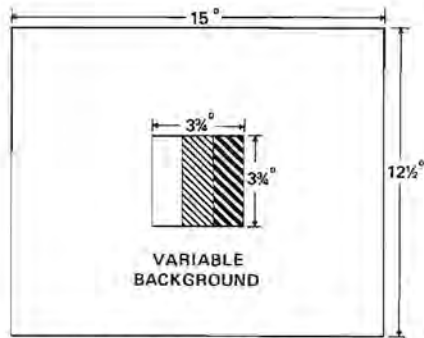


Fig. 6. Diagram of the video display for bisection experiments. The computer set the high luminance (unmatted rectangle left of center) and the low luminance (rectangle identified by heavy lines), and the observer selected the luminance of the middle area (thin lines) so that the lightness of this area appeared midway between the lightnesses of the two adjacent areas. The four different backgrounds shown at the bottom of Fig. 5 were inserted into the surrounding region.

ously. We presented the stimuli in a dark room on a Conrac 5411 television monitor driven by a computer-controlled image processor. In these experiments the observer varied the luminance of one area in the display by rotating a track ball linked to the computer. With these targets the bisections were done using three adjacent uniform rectangular areas located at the center of the display (see Fig. 6). The targets subtended 15-by-12.5 deg, and each of the three central areas subtended 1.25-by-3.75 deg. The viewing distance was 1 m; at this distance the observer could not resolve the raster lines on the display. The luminance of the high-luminance areas was 38 cd m^{-2} in targets A and D and 58 cd m^{-2} in targets B and C.

We provided white and black test areas and defined their lightnesses to be 9.0 and 1.0, respectively. The luminance of the white area was equal to that of the surround in target A. We asked the observer to select the seven additional intermediate lightnesses by a bisection procedure. In this procedure we presented lightnesses of 9.0 and 1.0 in the areas to the left and the right of the center of the target, and the observer rotated a track ball (computer input device) to vary the luminance of the central area to appear middle gray (lightness value, 5.0). The chosen luminance was presented at the right position in place of the black, and the observer selected a new luminance to bisect the lightnesses of 9.0 and 5.0. The luminance chosen as having a lightness of 5.0 was then presented at the left and black at the right, and the observer selected the lightness of 3.0. This process continued until all seven selections were made. At the conclusion of all the trials, the chosen digital image values were presented at the display in sequence, and the corresponding luminances were measured with a telephotometer and entered into the computer. We followed this procedure with five observers for each of the four targets. The number of trials ranged from six to twelve per observer. The ages of the observers ranged from 20 to 35 years.

Since the maximum luminance of the video display was much lower than the maximum luminance of the transmission target, the pupil of the eye was more dilated for these experiments. We estimated from Ref. 10 a pupil size of 3.9 mm for this level of luminance; accordingly, we performed the scatter calculation with the data of Vos *et al.*⁷ for the 3.8-mm pupil. The values of scatter-corrected luminance were taken in the

same manner as for the target in Fig. 1: Each value is the average of the luminances at four points on the principal diagonals midway between the center and the four corners of the areas at the center of the targets.

Results

The average bisection data for all observers for the four different backgrounds are shown in Fig. 5. In the upper graph we plot the averages of the logarithm of relative luminance of the target. The lower graph shows the averages of the logarithm of the calculated scatter-corrected luminances. In both graphs the horizontal axis is lightness; the vertical axis is the logarithm of the luminance normalized to the maximum on each target. The data from targets A, B, C, and D are plotted with the respective letters. The upper graph shows that bisection lightness experiments differ depending on the surround, as shown by Wyszecki and Stiles.¹² The bisection data from target D with a predominantly dark surround are reasonably well fitted by a straight line. The limited contrast range of the television tube prevents the luminance of the darkest areas in target A, with the full high-luminance surround, from being as low as those of the darkest areas in targets B, C, and D. The significant fact is that the curves connecting the data and representing uniform lightness functions for targets A, B, and C are definitely not straight lines.

After the calculation to include scatter, we find that the curves of the logarithm of luminance versus lightness are much more nearly linear. The change in the shape of the uniform lightness scales and the increased separation follows from the fact that much more light scatters from the bright surrounds than from the darker surrounds. The calculation of scatter dramatically changes the shape of the curve for the bright background in A, whereas the predominantly dark surround in D generates almost no light, and hence the scatter calculation hardly changes the shape of the curve. In target D, scatter increases the relative luminance of the darkest area from 0.4 to 0.6%. In target A, scattered light from the bright surround increases the luminance of the darkest area from 1.0 to 4.5%. The data for B and C are intermediate between those of A and D. Both sets of data are essentially similar, and both fall approximately on a straight line. The differences between the curves for these two targets may result from the difference in proximity of the test areas to the high-luminance areas in the two surrounds. The data for B, in which the high-luminance areas are contiguous with the test areas, show greater deviation from a straight line. In particular, the upper half of the curve from middle gray to white more closely resembles the shape of the curve for A than the straight line representing B and C drawn in the lower graph of Fig. 5.

The underlying purpose of the study of scatter was to isolate contrast mechanisms affecting targets with different surrounds. By contrast mechanism we mean spatial interactions that occur after visual receptors. The intraocular media scatter light from bright areas into darker areas, thereby reducing the real contrast of the retinal image. Nevertheless, the contrast mechanism generates the darkest sensations in the cases of greatest amounts of scatter. The magnitude of the contrast mechanism is concealed in graphs of target luminance, such as the upper graph of Fig. 5. However, graphs of luminance, after correction for intraocular scatter (lower graph of Fig. 5), show that there are much greater differences

in sensations generated by equal relative luminances as a function of the surround. For instance, the lowest sensation of black in a white surround (A) is generated by a relative luminance of 4.5%; in the dark surround (D), a relative luminance of 4.5% is seen with a lightness of 4.3. In the intermediate surrounds, 4.5% relative luminance has lightnesses of 3.1 and 3.5

We computed the intraobserver standard deviations of the logarithm of the relative luminances selected for each target by each observer; and for comparison we computed the interobserver standard deviations. The intraobserver standard deviations, although computed from fewer data, are typically smaller than the interobserver standard deviations because of consistent differences in mean levels of luminance chosen by individual observers. There are 35 intraobserver standard deviations per target: 5 observers with 7 selections of lightness from 2.0 to 8.0. The averages of these intraobserver standard deviations are 0.081, 0.103, 0.102, and 0.100 for targets A, B, C, and D, respectively. The standard deviations are typically largest for the first of the seven choices (lightness equal to 5) and smallest for the extreme values of luminance (lightness equal to 2 or 8). The averages of the five standard deviations for lightness equal to 5 are 0.110, 0.125, 0.129, and 0.151 for targets A, B, C, and D, respectively.

There are seven interobserver standard deviations per target: one for each value of lightness from 2.0 to 8.0. By averaging these seven, we obtained average interobserver standard deviations for the four targets. These values are 0.143, 0.178, 0.177, and 0.209, respectively. The interobserver standard deviations for lightness equal to 5 are 0.196, 0.213, 0.217, and 0.271.

Magnitude Estimation

A subtle issue is raised by plotting all four curves of Fig. 5 on a single graph. These four lightness scales, for targets A, B, C, and D, were derived by four independent lightness bisection experiments. An additional experiment is necessary to determine whether the white sensations are the same and whether the black sensations are the same on the four different backgrounds. In other words, if the horizontal axes are in fact the same, then the white area in the white surround will have the same sensation as the white area in the black surround. The rationale of this experiment is simply to justify plotting all four curves on a single graph instead of on four graphs.

We set up an experiment in which we gave observers references of both white and black sensations. We asked each observer to make a magnitude estimation of the white, the variable gray, and the black sensations found in the four targets.

We set the rectangular areas to the left and the right of the central areas on the four targets to maximum luminance (white) and minimum luminance (black), respectively; and we defined the white and the black areas on target A as having lightnesses of 9.0 and 1.0, respectively. The observer made the display alternate between target A and each of the other three targets in turn and estimated the lightnesses of the three areas at the centers of each of B, C, and D using the two lightnesses (9.0 and 1.0) assigned on target A as references. In each of the ten trials a different gray level was used in the central areas of both target A and the test target. We included the gray areas to relieve the monotony of estimating

the lightnesses of the white and black areas. All five observers had ten trials for each of the three targets. The thirty trials for each observer were presented in the same randomly chosen order, and the resulting estimates of lightness were averaged over the five observers.

The question was whether the observers estimated the white areas in targets B, C, and D and the black areas in B, C, and D to be significantly different from the white and the black (with lightnesses of 9.0 and 1.0) in target A. The average lightnesses for the white and the black on B were 8.91 ± 0.19 and 1.03 ± 0.11 ; they were 8.92 ± 0.20 and 0.96 ± 0.11 on target C; and they were 8.96 ± 0.17 and 0.96 ± 0.15 on D. Thus there is no significant difference between the lightnesses of the lightest and darkest areas from target to target, and accordingly we are justified in plotting the data for the four targets on a single lightness axis in Fig. 5.

DISCUSSION

Only in special cases do we find that lightness is a simple function of luminance. With natural scenes in generally nonuniform illumination, with Mondrian displays in nonuniform illumination,^{13,14} with gray squares on large white and black surrounds,¹⁵ with Mach bands,¹⁶ with gradients of luminance,^{17,18} and with changes in the overall intensity of illumination,¹⁹ lightness cannot be expressed as a function of luminance at a point. Lightness at any one point is a function of the luminance at that point and the luminance at all other points. Nevertheless, it is of interest to study the special case of fixed geometry in which the luminance of only one area is varied. This special case allows us to study the functional form of luminance versus lightness.

The significance of our results is twofold. All five cases studied involved uniform areas and uniform surrounds, and our results show that in these circumstances the sensations of lightness are proportional to the logarithm of scatter-corrected luminance for different backgrounds and that the constant of proportionality depends on the specific target. The reason that previous experiments have shown lightness to be a power function of luminance is that the scattering of incident light within the ocular media has not been considered. Models of lightness under these uniform conditions need incorporate only simple logarithmic functions of luminance. Second, the fact that different backgrounds yield lightness scales with different slopes shows that lightness is a function of both luminance at a point and spatial interactions with other points in the field of view. In other words, correcting for intraocular scatter does not diminish, but rather increases, the need for understanding spatial interactions that generate lightness.

Let us make a distinction between two kinds of contrast. The first, physical contrast, is a measure of the magnitude of luminance differences in an image. The second, apparent contrast, is a measure of the magnitude of the sensation differences in an image. Consider the classic example of simultaneous contrast. Here we have two identical gray patches: one in a white surround and one in a black surround. If we examine the image on the retina in terms of physical contrast, the gray patch in the white surround has a higher retinal luminance. The high-luminance, white surround scatters light into the nearby lower-luminance gray patch. Little light is scattered into the patch in the black surround.

Nevertheless, in terms of apparent contrast the white surround makes the gray patch appear darker rather than lighter. The visual or neural contrast mechanism that makes the low-luminance areas appear darker in bright environments more than compensates for the reduced physical contrast caused by intraocular scatter. The classical simultaneous contrast phenomenon is the remainder left by a lack of perfect cancellation of two opposing phenomena: physical light scattering and a neural contrast mechanism. Two such different types of mechanism cannot exactly compensate for each other in all possible images. Nevertheless, neural contrast tends to compensate for intraocular scatter and, in some cases, even overcompensates. This cancellation effect tends to make objects of a given relative luminance appear to be of a constant lightness. These observations also show that studies of neural contrast mechanisms should include consideration of intraocular scatter.

ACKNOWLEDGMENTS

The authors appreciate the assistance of Karen L. Houston and Jonathan A. Frankle in conducting the experiments and preparing the manuscript.

This paper was presented at the annual meeting of the Optical Society of America at Rochester, New York, October 9–12, 1979.

* Present address, The Rowland Institute for Science, Inc., 100 Cambridge Parkway, Cambridge, Massachusetts 02142.

REFERENCES

1. A. E. O. Munsell, L. L. Sloan, and I. H. Godlove, "Neutral value scales. I. Munsell neutral value scale," *J. Opt. Soc. Am.* **23**, 394–411 (1933).
2. J. H. Ladd and J. E. Pinney, "Empirical relationships with the Munsell value scale," *Proc. Inst. Radio Eng.* **43**, 1137 (1955).
3. L. G. Glasser, A. H. McKinney, C. D. Reilley, and P. D. Schnelle, "Cube-root color coordinate system," *J. Opt. Soc. Am.* **48**, 736–740 (1958).
4. S. S. Stevens and J. C. Stevens, *The Dynamics of Visual Brightness*, Harvard University Psychological Project Rep. PPR-246 (Harvard University, Cambridge, Mass., 1960).
5. D. Jameson and L. M. Hurvich, "Complexities of perceived brightness," *Science* **133**, 174–179 (1961).
6. C. C. Semmelroth, "Prediction of lightness and brightness on different backgrounds," *J. Opt. Soc. Am.* **60**, 1685–1689 (1970).
7. J. J. Vos, J. Walraven, and A. van Meeteren, "Light profiles of the foveal image of a point source," *Vision Res.* **16**, 215–219 (1976).
8. J. J. McCann, E. H. Land, and S. M. V. Tatnall, "A technique for comparing human visual responses with a mathematical model for lightness," *Am. J. Optom.* **47**, 845–855 (1970).
9. A. van Meeteren, "Calculations on the optical modulation transfer function of the human eye for white light," *Opt. Acta* **21**, 395–412 (1974).
10. S. H. Bartley, "The psychophysiology of vision," in *Handbook of Experimental Psychology*, S. S. Stevens, ed. (Wiley, New York, 1951), Chap. 24, Fig. 64.
11. However, the scatter function diminishes so rapidly within a few minutes of the peak that 1' samples are too coarse. The scatter function has been preprocessed at a resolution of 1" for small angular distances from the peak to give precise measures of the integrated fractions of energy scattered from 1' areas at these distances.
12. G. Wyszecki and W. S. Stiles, *Color Science* (Wiley, New York, 1967), Sec. 6, Fig. 6.1.
13. E. H. Land, "The retinex theory of colour vision," *Proc. R. Inst. G. B.* **47**, 23–58 (1974).
14. E. H. Land and J. J. McCann, "Lightness and retinex theory," *J. Opt. Soc. Am.* **61**, 1–11 (1971).
15. M. E. Chevreul, *The Principles of Harmony and Contrast of Colours and Their Applications to the Arts* (Reinhold, New York, 1967).
16. F. Ratliff, *Mach Bands: Quantitative Studies on Neural Networks in the Retina* (Holden-Day, San Francisco, 1965).
17. J. J. McCann, R. L. Savoy, J. A. Hall, Jr., and J. J. Scarpetti, "Visibility of continuous luminance gradients," *Vision Res.* **14**, 917–927 (1974).
18. J. J. McCann, "Visibility of gradients and low spatial frequency sinusoids: evidence for a distance constancy mechanism," *Photogr. Sci. Eng.* **22**, 64–68 (1978).
19. D. Katz, *The World of Colour* (Kegan Paul, Trench, Trubner, London, 1935).